Migration error in transversely isotropic media

Tariq Alkhalifah and Ken Larner

ABSTRACT

Most migration algorithms today are based on the assumption that the earth is isotropic, an approximation that is often not valid and thus can lead to position errors on migrated images. Here, we compute curves of such position error as a function of reflector dip for transversely isotropic (TI) media characterized by Thomsen's anisotropy parameters δ and ϵ. Depending on whether the migration velocity is derived from stacking velocity or vertical root-mean-square (rms) velocity, we find quite contrary sensitivities of the error behavior to the values of δ and ϵ. Likewise error-versus-dip behavior depends in a complicated way on vertical velocity gradient and vertical time, as well as orientation of the symmetry axis. Moreover, error behavior is dependent on just how δ and ϵ vary with depth. In addition to presenting such error curves, we show migrations of synthetic data that exemplify the mispositioning that results from ignoring anisotropy for P-wave data.

When migration is done using velocities derived from stacking velocity and when medium velocity increases with depth at rates typically encountered in practice, δ alone is sufficient to describe the position error. This is fortunate since the value of δ, unlike ϵ, can be obtained from combined vertical seismic profile (VSP) and surface seismic data. In contrast, when the migration velocity is obtained from the vertical rms velocity, the position errors depend strongly on ϵ, suggesting the importance of having an accurate estimate of ϵ when using an anisotropic migration algorithm.

INTRODUCTION

Invariably, the earth's crust is anisotropic. Nevertheless, through the years, processing of seismic data has seldom taken anisotropy into consideration. Conventional processing seemed to work well, and taking anisotropy into consideration was thought to be complicated, slow, and costly. It is likely, however, that ignoring anisotropy has lead to errors that have been either unrecognized or attributed to acquisition and processing problems. Such errors are usually left unmeasured and untreated.

Larner and Cohen (1993) have studied the mispositioning of imaged reflectors that results when, as is typically done in practice, conventional P-wave data from transversely isotropic (TI) media are migrated with an algorithm that ignores anisotropy. The media they studied had linear velocity variation with depth, had a vertical symmetry axis for the transverse isotropy, and were factorized anisotropic inhomogeneous (FAI; Červený, 1989). That is, all ratios among the various elasticity parameters were independent of position. Moreover, they limited their study to the four examples of TI media studied by Levin (1990) and listed in Table 1. They found highly variable dependence of the behavior of lateral position error versus reflector dip upon the velocity gradient and vertical reflection time.

While their curves were interesting and might qualitatively explain apparent accuracy of migration in practice, those results have no ready explanation in terms of current knowledge about anisotropy. Moreover, while more general than those studied in the past, the model used by Larner and Cohen had a number of limitations that are lifted in this follow-up study. While retaining the restriction that the medium be TI, we allow the symmetry axis to be tilted from vertical, and we consider departures from FAI media. Also, rather than limit study to four specific media, we characterize the anisotropy of the media more generally in terms of the Thomsen (1986) parameters δ and ϵ [see equations (1) and (2), below], and V_s/V_p, where V_p and V_s are

the P-wave and S-wave velocities along the symmetry-axis direction. We find that migration errors are quite insensitive to V_s/V_p, even for media not considered weakly anisotropic. (Here, and throughout the paper, we consider P-wave data only.) With this parameterization, we can gain understanding of the results for the four media studied by Larner and Cohen in terms of the δ and ϵ values for those media. Also, with this parameterization, we can efficiently study media having a wide range of anisotropy.

Following the general study of error-versus-dip curves, we generate synthetic data for TI models with steep reflectors, and see the action of isotropic time migration on those data. Such sample migration tests highlight the dependence of position error on symmetry-axis direction, as well as difficulties in assessing migration error in practice.

Paralleling Larner and Cohen (1993), we first generate two-way traveltimes corresponding to zero-offset P-wave data from point scatterers, by ray tracing in a TI medium with constant velocity gradient (Alkhalifah, 1993). Larner and Cohen considered only FAI, TI media with constant velocity gradient so as to take advantage of the analytic solution of Shearer and Chapman (1988) for ray tracing in such media. We generalize to TI media that are not factorized anisotropic inhomogeneous by perturbing the FAI traveltimes (Alkhalifah, 1993), patterned after the perturbation ideas of Červený and Filho (1991). Once we have generated the diffraction curves, we then simulate migration of points along these diffraction curves with an algorithm that computes diffraction times for an isotropic medium with velocity variation equal to that for the vertical velocity in the TI medium. The only source of error in the simulated migration should be the failure to honor anisotropy in the migration.

Following Larner and Cohen (1993), we study the dimensionless lateral distance $\Delta\tilde{y}$ between the incorrectly imaged reflector position and the true position of the reflector,

$$\Delta\tilde{y} = \frac{\Delta y}{\lambda_d},$$

where Δy is the error in horizontal distance, and λ_d is the horizontal wavelength

$$\lambda_d = \frac{1}{f_d p},$$

with f_d a selected "dominant" frequency, and p the slope of the unmigrated reflection. Positive position errors imply undermigration, and negative position errors imply overmigration. The reference dominant frequency used here is 30 Hz.

Repeating, here we consider only a velocity gradient in the vertical direction, and only 2-D propagation in the vertical plane perpendicular to strike, but allow general orientation ψ of the symmetry axis within the propagation plane. The velocity gradient used in most tests is 0.6 s^{-1}, which we judge to be a sufficiently representative value for the subsurface, considering that the constant gradient is itself a simplification. Also, in most of the tests, the depth D of the reflection point is 3000 m, and the vertical root-mean-square (rms) velocity $V_{\rm rms}$ to that point is 3000 m/s; thus the vertical (migrated) time to the reflection point is $t_m = 2D/V_{\rm avg} \approx 2D/V_{\rm rms} = 2$ s, where $V_{\rm avg}$ is the vertical average velocity. With the exception of the vertical time, these are values generally used by Larner and Cohen (1993) in their study of migration error for vertical axis of symmetry. In all cases where migration velocity is based on the stacking velocity, the $T^2 - X^2$ analysis is done over a spreadlength X equal to the depth D of an assumed horizontal reflector. We also consider, at first, just factorized transversely isotropic (FTI) media; that is, media in which all ratios among the elastic coefficients for TI media (therefore, V_s/V_p, δ, and ϵ) are independent of position. Later, we lift this restriction.

VELOCITY

Migration velocity

Commonly, the interval velocities required to migrate field data are derived from stacking velocity. In horizontally layered, isotropic media, the stacking velocity usually approximates the vertical rms velocity with acceptable accuracy. This is not so, however, for anisotropic media. The velocity variation as a function of direction causes the best-fit stacking velocity obtained from conventional velocity analysis to differ from the vertical rms velocity, even for small offsets in horizontally layered media. These differences are highlighted by Thomsen (1986) for homogeneous TI media, and by Larner and Cohen (1993) for TI media with a vertical axis symmetry and constant vertical velocity gradient. Larner and Cohen showed that position errors are smaller when stacking velocity, as opposed to vertical rms velocity, is used to obtain velocities for isotropic time migration, as is typically done in practice.

Figure 1 shows the dip-dependence of the lateral position error for four angles ψ of the symmetry axis with the vertical, using for the migration either the vertical rms velocity (solid lines) or the stacking velocity (dashed lines). Here, and throughout the remainder of the paper, the term stacking velocity will pertain to finite-spreadlength normal-moveout (NMO) correction velocity for horizontal reflectors. Positive ψ corresponds to axis of symmetry tilted toward the normal to the dipping reflector, and negative ψ means that it is tilted away from the normal. Here, for both shale-limestone (black lines) and Cotton Valley shale (gray lines), two of the media with properties listed in Table 1, migration errors for $\psi = 30$ degrees are smaller when migration velocity is derived from vertical rms velocity than when it is derived from the stacking velocity. We attribute this to the asymmetric and laterally shifted diffraction curves when the symmetry axis departs from vertical. In an isotropic medium, lateral velocity variation is needed in order for diffraction curves

to be asymmetric and shifted. Not so for a tilted symmetry axis. Moreover, where velocity varies with depth only, moveout in common-midpoint (CMP) gathers does not change from one gather to another. Thus, with a tilted symmetry axis, we cannot expect a good fit of the diffraction curve for isotropic medium to that of a TI medium, so we have no reason to expect stacking velocity to be a better source of migration-velocity information than is vertical rms velocity.

Velocity analysis

To obtain the stacking velocity appropriate for horizontal reflectors, one usually attempts either to apply velocity analysis to CMP gathers that contain reflections from horizontal reflectors or to account for the dipping reflectors (by either including an appropriate "dip-correction" factor or performing velocity analysis on dip-moveout-processed data). Thomsen (1986) showed that small-offset stacking velocity differs from the vertical velocity in a homogeneous TI medium with vertical axis of symmetry. The ratio of these two quantities depends solely on Thomsen's parameter δ. The same relationship holds for vertically inhomogeneous media, with constant δ, provided that the vertical velocity is replaced by the vertical rms velocity (Hake, et al., 1984).

Table 2 contains the ratio of the stacking velocity to the vertical rms velocity ($V_{\rm stack}/V_{\rm rms}$) for horizontally layered versions of the same TI media shown in Table 1, but here the axis of symmetry is not limited to the vertical. Given the moveout symmetry within CMP gathers, the sign of the angle of the symmetry axis is immaterial. Note, in Table 2, that the angle-dependence of the velocity ratio is greatest for the Cotton Valley shale, whereas it is quite small for the shale-limestone. These differences are related to a large value of the Thomsen parameter δ for the Cotton Valley shale, whereas it is zero for the shale-limestone (see Table 1).

MIGRATION ERRORS

Rather than study errors for specific media (i.e., Cotton Valley shale) as Larner and Cohen (1993) did, hereafter we use Thomsen's (1986) parameters to identify the TI media. As we shall see, error behavior is well characterized by certain of these parameters. The two key Thomsen parameters for P-waves are δ, which describes near-vertical velocity variation, and ϵ, which involves just the ratio of the horizontal to vertical velocity for a TI media with vertical symmetry axis. In terms of the elastic coefficients, C_{ij}, these two dimensionless parameters are

$$\delta = \frac{(C_{13} + C_{44})^2 - (C_{33} - C_{44})^2}{2C_{33}(C_{33} - C_{44})}, \tag{1}$$

$$\varepsilon = \frac{C_{11} - C_{33}}{2C_{33}}. \tag{2}$$

These parameters, along with the P-wave velocity V_p and S-wave velocity V_s in the symmetry-axis direction are sufficient to describe anisotropic behavior of P-waves in a TI medium. Negative δ (as exemplified by Taylor sandstone, listed in Table 1) implies that the velocity will initially decrease away from the symmetry direction. In contrast, negative ϵ describes a medium where velocity in the symmetry direction exceeds that in the isotropy plane, a rare occurrence.

Dependence on anisotropy

Figure 2 shows lateral position error as a function of reflector dip keeping $\delta = .1$, $\epsilon = .2$ for the left plot, and $\delta = .1$, $\epsilon = 1.5$ for the right plot, and using the same $V_p(z)$ for all the curves, where z is depth. The only parameter changed from one curve to another within each plot is the S-wave velocity, V_s, such that V_s/V_p ranges from 0.3 to 0.7, a wide range that covers all cases of practical interest. Differences among the curves are insignificant up to about 80-degree reflector dip. Rays must pass the turning point before any differences of significance are realized for even unusually strongly anisotropic media (e.g., $\epsilon = 1.5$). For relatively moderate anisotropy (e.g.,

$\epsilon = 0.2$) the position errors are relatively small (less than four wavelengths at 120-degree dip), and differences among the curves are insignificant up to 120 degrees. Similar behavior holds for the range of practical choices for δ (not shown here). Therefore, for P-waves, the two parameters, δ and ϵ, are sufficient to characterize velocity variations in most TI media (Tsvankin and Thomsen [1993] found the same behavior for homogeneous media). Here, as elsewhere Thomsen's parameters are a convenient set for characterizing even TI media that are not necessarily "weakly anisotropic."

Figure 3 shows lateral position error as a function of reflector dip for a wide range of TI media represented by different combinations of δ and ϵ, with vertical velocity gradient 0.6 s^{-1} and vertical axis of symmetry. The reflector depth D and vertical rms velocity $V_{\rm rms}$ are chosen so that the reflection point is at a migrated time $t_m = 2D/V_{\rm rms} = 2$ s. Here, following Larner and Cohen (1993), we use the stacking velocity to derive migration velocity. As a result, the position errors are not zero when $\delta = \epsilon = 0$ (isotropic medium) because moveout is nonhyperbolic for the inhomogeneous medium.

Figure 3 shows that when using the stacking velocity as the basis for the migration process, the influence of δ on the position error is insignificant for dip less than 50 degrees, but is considerably greater than that of ϵ, for steep reflectors. This is evident in the closeness of curves within each of the left-column plots of Figure 3, as opposed to the branching out of curves in the right column of Figure 3. When stacking velocity, as opposed to rms velocity, is used to derive velocity for migration in a TI medium, we expect that we have corrected for the influence that δ has on the traveltime. This expectation is based on the following: δ controls near-vertical propagation velocities, and stacking velocity is obtained from a best fit to moveout for reflectors over a range of angles near vertical This expectation seems to be satisfied for small to moderate dip (i.e., less than about 50 degrees).

Also, as Figure 3 suggests, when using velocities derived from the stacking velocity in migrating seismic data, δ controls the sign of the position error for steep reflectors. For negative δ, steep reflectors will generally be undermigrated; for positive δ, they will generally be overmigrated. This observation, however, cannot be generalized to vertical migrated time other than $t_m = 2$ s (see Figure 6). This sensitivity of error to δ implies that δ largely governs the expected position error for steep reflectors. This is fortunate since the value δ, unlike ϵ, can be obtained with relatively good accuracy from seismic data (e.g., analysis of vertical seismic profile data, combined with stacking velocity). These observations hold for vertical velocity gradient greater than about 0.5 s^{-1}, as was the case in Figure 3. However, as seen in Figure 4, for vertical velocity gradient smaller than about 0.5 s^{-1}, ϵ begins to play a larger role in position errors. For large gradient, such as $k = 1.0$ s^{-1}, ϵ tends not to have any influence on the position error. Where velocity increases substantially with depth, the curved rays spend more time at near vertical, and thus δ has a relatively larger influence on the traveltime than when the gradient is small and thus raypaths are less curved. Note also in Figure 4, for the combination of $k = 0$ s^{-1} and $\epsilon = \delta = 0.05$ (homogeneous, elliptically anisotropic), the position errors for all dips equal zero. This result, which holds for all homogeneous, elliptically isotropic media, implies that use of the stacking velocity for isotropic time migration in such media is equivalent to doing time migration with an algorithm that honors elliptical anisotropy. The conversion from time to depth, however, would require use of the vertical rms velocity rather than the stacking velocity.

Figure 5 is the same as Figure 3, except that this time the vertical rms velocity is used to obtain the migration velocities. Although Larner and Cohen (1993) favored use of stacking velocity (obtained for horizontal reflectors) to derive migration velocities, our studies lead us to believe that neither source of migration velocity information— stacking velocity nor vertical rms velocity— is the universally proper

choice for steep reflectors (reflectors with dip greater than about 50 degrees). Since anisotropy is ignored in the migration, neither choice can be correct. Interestingly, the two choices lead to contrasting error behavior. One difference is that, unlike the stacking-velocity case, here we are using a single vertical rms velocity in the migration for all the curves. For Figure 3, stacking velocity differed for each choice of δ and ϵ. In comparing the plots in Figure 5 with those in Figure 3, δ and ϵ seem to have interchanged roles in influencing the position errors. When stacking velocity was used, δ was the major factor governing imaging accuracy of steep reflectors. When using the vertical rms velocity for the migration, now ϵ plays the larger role. Also, where δ has little influence on errors for small dip in Figure 3, ϵ has little influence in that region in Figure 5.

In Figure 5, when $\delta = \epsilon = 0$ (isotropic medium) the error is zero for all dips. This supports the interpretation that errors shown in these plots are attributable solely to anisotropy. For small ϵ (upper right) the position errors are low and possibly tolerable over a wide range of δ. Given the large sensitivity of position error to ϵ when the vertical rms velocity is used in isotropic migration, we infer that one should not go to the effort of using a migration algorithm that honors anisotropy unless ϵ is well estimated. This contention further suggests that the practice of equating ϵ to δ and doing migration based on elliptical anisotropy, as is often done when the actual value of ϵ is unknown, might lead to erroneous migrations, especially for reflector dip greater than about 50 degrees.

Furthermore, numerical experiments with anisotropic migration by Gaussian beams (not shown here) suggest that error curves such as those in Figure 5 hold as well when data are migrated with an anisotropic algorithm, but with incorrect values for δ and ϵ. Specifically, any curve governed by δ and ϵ in Figure 5 remains generally unchanged when data from media characterized by δ^o and ϵ^o are migrated using the parameters $\delta^1 = \delta^o - \delta$ and $\epsilon^1 = \epsilon^o - \epsilon$. Thus, prior to re-migrating data for which improved

information on δ^o and ϵ^o become available, one can get a general idea of the errors that have resulted in migration that uses δ^1 and ϵ^1.

Dependence on vertical time

From this point on, only stacking velocity is used to compute migration velocities. Stacking velocity is the more widely used velocity in migration when the presence of anisotropy is ignored.

Larner and Cohen (1993) showed that the vertical time, $t_m = 2D/V_{\text{avg}}$, is sufficient to describe the position-error dependency on depth and velocity. That is, they showed that when the depth D and vertical average velocity V_{avg} vary such that t_m remains unchanged, the position error is also unchanged.

Figure 6 shows the behavior of lateral position error for t_m ranging from 1 to 4 s. As noted by Larner and Cohen, the migrated section tends to shift from undermigration toward overmigration with increasing t_m. Above, we saw that for $t_m = 2$ s, positive δ generally produces overmigrated images, where negative δ produces undermigrated images. However, for other values of t_m, the simple relation concerning positive and negative δ generalizes to a tendency toward greater migration with increasing numerical value of δ.

Dependence on symmetry-axis direction

Figure 7 shows the position errors for a respectable range of angles ψ of the symmetry axis with the vertical. Note that the dependency of the error curves on δ is highly influenced by the axis orientation. When $\delta \approx 0.05$, the dependence of position error on ψ is relatively small. In contrast, when $\delta = -0.1$ (solid black lines), ψ has large influence on the position errors. This relative behavior suggests that the sensitivity of errors to ψ is directly related to the amount by which velocity changes with direction. Clearly, the orientation of the symmetry axis greatly influences errors.

Fortuitously, the errors could be small for all dips, for some combinations of δ, ϵ, and ψ (e.g., when $\psi = -10$ degrees and $\delta = 0$, for $\epsilon = 0.1$ and $k = 0.6\,\mathrm{s}^{-1}$, as in Figure 7).

Dependence on anisotropy variation

Here, we lift the constraint that the medium be factorized transversely isotropic (FTI) and allow δ and ϵ to vary slowly with depth. To do this, we compute traveltimes for a generally TI medium via perturbation of the traveltimes obtained for an FTI medium (Alkhalifah, T., 1993, Center for Wave Phenomena Report, CWP-129, Colorado School of Mines). We shall consider two cases: (1) a medium that is isotropic at the surface and slowly varies to become TI at the reflector, and (2) just the reverse. For both cases, $\psi = 0$, and the stacking velocity is used to obtain migration velocity.

Figure 8 shows lateral position errors for two different degrees of variation in anisotropy. Each curve pertains to a medium that is isotropic at the surface, steadily changing with depth to become more severely TI at the reflector. For the left plot, ϵ increases linearly with depth from zero at the surface to 0.1 at the reflector depth of 3000 m. For the right plot, ϵ increases linearly from zero at the surface to 0.2 at the reflector. Each curve represents a different constant gradient in C_{44}/C_{33}, such that δ increases nonlinearly from zero at the surface to the values shown in Figure 6 at the reflector.

In FTI media, δ had a large influence on the position error, as seen in Figure 3, but, this influence is diminished in Figure 8. Specifically, note that the curves are not as spread out here as they were in the right column of Figure 3. This may be related to the fact that the ray is at near-vertical in the shallower part of the medium, where δ is small and thus has little influence on velocity.

For Figure 9, the model variation is opposite to that in Figure 8. This time the medium is TI at the surface, and steadily changes to being isotropic at the reflector.

Here, for the left plot, ϵ decreases linearly with depth from 0.1 at the surface to zero at the reflector depth of 3000 m. For the right plot, ϵ decreases linearly from 0.2 at the surface to zero at the reflector. Again, each curve represents a different constant gradient in C_{44}/C_{33}, such that δ decreases nonlinearly from the values shown in Figure 6 at the surface to zero at the reflector. The error-curve pattern is essentially opposite to that in Figure 8. Now, δ has the upper hand in controlling migration position errors, and ϵ has its influence greatly diminished.

Again, differences in the behavior of the error curves in Figures 8 and 9 are controlled largely by the size of vertical velocity gradient (k=0.6 s^{-1} in these figures). For smaller gradient the two figures would show smaller difference.

SYNTHETIC DATA EXAMPLES

To this point, we have been showing curves of position error for a wide variety of situations. Let us now see how these errors are manifested in the imaging of synthetic data. The zero-offset data (not shown here) were generated using a Kirchhoff-summation type algorithm for TI media (Alkhalifah, T., 1993, Center for Wave Phenomena Report, CWP-129, Colorado School of Mines), and we use here the time-wavenumber (t-k) migration algorithm of Hale (1991, Center for Wave Phenomena Annual Report, CWP-107, Colorado School of Mines). This isotropic time-migration algorithm was chosen largely because it preserves the amplitudes of the vertical reflectors in isotropic media.

Figure 10 shows a model containing horizontal reflectors with dipping segments having dips ranging from 30 to 90 degrees on both sides. The medium has the properties of Taylor sandstone ($\delta = -0.035$ and $\epsilon = 0.11$) with a vertical velocity $v(z)$=2000+0.6z m/s. Figure 11 shows three sections, all migrated using the isotropic t-k algorithm of Hale, with velocities calculated from the stacking velocity. In (a) the medium is isotropic, so the migration is accurate for all dips, with only a slight

overmigration related to the small difference between the stacking velocity and the actual vertical rms velocity in a vertically inhomogeneous medium. In contrast, the steep portions are erroneously migrated for the Taylor sandstone TI medium, with errors largely influenced by the orientation of the symmetry axis. The arrows in Figure 7 point to the approximate errors expected for the Taylor sandstone having the symmetry-axis directions used in Figure 11. The differences in ϵ (0.11 for the Taylor sandstone and 0.1 in Figure 7) are insignificant since, as seen above, ϵ has little influence on position error when stacking velocity is used. At migrated time $t_m = 2$ s in Figure 11, the horizontal position errors reflect, in general, the results obtained from the curves in Figure 7. However, those curves could not show the artifacts seen near the reflector corners in the migrated data. Note also that the 90-degree reflector in (c) appears overturned. Also, the horizontal segments are shifted slightly to the right, consistent with expectation from the modeling results in Alkhalifah (1993, Center for Wave Phenomena Report, CWP-129, Colorado School of Mines).

Figure 11 is representative of fault-like structures, where the dip changes abruptly at the fault. In this circumstance, anisotropy-generated errors are clearly observed, and practical measures can be taken to correct for the errors; e.g., the migration velocity function can be altered to improve the "look" of the data, or perhaps an anisotropic migration algorithm can be used. However, often errors due to ignoring anisotropy can pass unnoticed. An example of this problem is the situation where reflectors have continuously varying dip similar to that in bedding upturned against a steep salt-dome flank, as depicted in Figure 12. Figure 12 shows migrated sections for TI media with (a) $\delta = 0.1$, $\epsilon = 0.15$ and $\psi = 0$, and (b) $\delta = -0.1$, $\epsilon = 0.1$ and $\psi = 0$. The dotted lines show the true location of the salt-dome flank. With anisotropy ignored, the migrated images look plausible in both cases (i.e., little or no crossing of reflections), yet both are incorrect and differ substantially from one another.

In isotropic $v(z)$ media, conversion from time to depth is accomplished with use of vertical average velocity computed from stacking velocity under the assumption that stacking velocity approximates the vertical rms velocity. For TI media with vertical symmetry axis, such a computation would lead to an erroneous estimate for the vertical average velocity because stacking velocity can differ substantially from vertical rms velocity. An approximation for the depth error that results when the stacking velocity is used for computation of the average velocity is

$$D_{\text{shift}} \simeq \left(\frac{V_{\text{stack}}}{V_{\text{rms}}} - 1\right) D,$$

where D is the true depth of the reflector. Time-depth misties due to anisotropy are common in shale formations (Banik, 1984). Such errors can be corrected by obtaining an estimate of δ for the medium. Then, the vertical rms velocity can be calculated from the limiting stacking velocity as $X/D \rightarrow 0$ (Thomsen, 1986). In a $v(z)$ medium, depth migration is equivalent to time migration followed by a time-to-depth conversion. Therefore, the depth error resulting from using the stacking velocity in the conversion is comparable to that when depth migration is done with velocities derived from the stacking velocity. (Depth migration would have the same lateral position errors indicated in the curves.) The depth-shift problem is similar to that described by VerWest (1989) for migration in elliptically anisotropic media, and could be similarly corrected with use, in effect, of different velocities for the migration and for the depth conversion, especially for near-horizontal reflectors.

Figure 13 shows a migrated image using an isotropic depth-migration algorithm for the model in Figure 10. The medium is Taylor sandstone, and the vertical velocity is $v(z)$=2000+0.6 z m/s. Because the velocity used in the migration process is the stacking velocity, all reflectors, but most obviously the horizontal ones, are imaged too deep (compare with Figure 10). In field data, these depth errors might not be recognized without some assessment of the anisotropy of the medium.

CONCLUSION

For the ranges of δ and ϵ studied here, an isotropic time migration using the stacking velocity would result in acceptable images for reflector dip less than about 50 degrees in laterally homogeneous media. This result should offer comfort to those concerned with errors in imaging that might arise from ignoring anisotropy for moderately steep structure. The need to take anisotropy into account increases rapidly, however, for dip beyond about 50 degrees. This conclusion holds for the wide range of anisotropic media studied here (i.e., for the large range of values of δ and ϵ studied).

Depending on whether the migration velocity is derived from stacking velocity or vertical rms velocity, we find quite contrary sensitivities of the error behavior to the values of δ and ϵ. In media with typical vertical velocity gradient (0.5 s^{-1} or greater) and $\psi = 0$, the value of δ largely governs the position errors for steep reflectors (dips greater than about 50 degrees) when using the migration velocity derived from stacking velocity. This is convenient, since δ is the anisotropy parameter most readily obtainable from seismic data. In addition, for such migration, most of the errors in TI media are associated with steep reflectors.

Our only explanation for the relatively small errors for dip less than about 50 degrees is that our velocity information was derived from fitting moveout over a range of angles near vertical, and δ is known to control the behavior of velocity at angles near vertical. In any case, the results hold for the large range of anisotropic media studied.

Interestingly, when the vertical rms velocity, which is independent of values of δ and ϵ, is used in the migration process, the value of ϵ largely governs the position errors, especially for steep reflectors and velocity gradient 0.5 s^{-1} or greater. Given the large sensitivity of position error to ϵ when the vertical rms velocity is the source of velocity information for isotropic migration, we infer that one should not go to

the effort of using a migration algorithm that honors anisotropy unless ϵ is properly estimated. This contention further suggests that the practice of equating ϵ to δ and doing migration based on elliptical anisotropy, as is often done when the actual value of ϵ is unknown, might lead to erroneous migration, especially for reflector dip greater than about 50 degrees because elliptical anisotropy is hardly typical of the subsurface. For vertical velocity gradients of 0.5 s^{-1} or more, if the value of ϵ is not well known we believe it is better to do isotropic migration with velocity derived from stacking velocity and use the value of δ to estimate the errors than to do migration based on an anisotropic algorithm.

The above conclusions pertain to media with vertical symmetry axis. Tilting of the axis adds yet more complication to migration-error behavior. Tilt in the orientation of the symmetry axis results in lateral shifts of imaged horizontal reflectors from their true positions, much as happens when time migration is used where overburden velocity varies laterally. Such tilt could be a factor of importance in the vicinity of salt-dome flanks.

Clearly, models with constant velocity gradient and FTI are simplifications of the true subsurface. The limitation to constant velocity gradient could readily be relaxed by a perturbation method similar to that used in going from FTI to general TI media. Despite the limitations of the models used here, analysis of position errors for these models should aid in understanding accuracy limitations in anisotropic media.

Unless we are imaging a fault or structure with sharp edges, many errors due to anisotropy pass by unnoticed, particularly given the latitude often exercised in choosing migration velocity, in practice. Clearly, the key to success in migration in the presence of anisotropy is the use of an algorithm that not only honors anisotropy, but also uses good estimates of the anisotropy parameters, δ and ϵ.

ACKNOWLEDGMENTS

We thank Ilya Tsvankin for his useful insights at critical stages of this study, especially his suggestion to parameterize the TI media in terms of Thomsen's parameters, and for his review of the manuscript. Financial support for this work was provided in part by the United States Department of Energy (this support does not constitute an endorsement by DOE of the views expressed in this paper) and by the members of the Consortium Project on Seismic Inverse Methods for Complex Structures at the Center for Wave Phenomena, Colorado School of Mines. Thanks are also due to KACST for financial support of Tariq Alkhalifah's study.

REFERENCES

Banik, N.C., 1984, Velocity anisotropy of shales and depth estimation in the North Sea basin: Geophysics, **49**, 1411-1419.

Červený, V., 1989, Ray tracing in factorized anisotropic inhomogeneous media: Geophys. J. Internat., **94**, 575–580.

Červený, V., and Simoes-Filho, I. A., 1991, The traveltime perturbations for seismic body waves in factorized anisotropic inhomogeneous media: Geophys. J. Internat., **107**, 219–229.

Hake, H., Helbig, K., and Mesdag, C.S., 1984, Three-term Taylor series for $t^2 - x^2$ curves over layered transversely isotropic ground: Geophys. Prosp., **32**, 828-850.

Larner, K. and Cohen, J., 1993, Migration error in factorized transversely isotropic media with linear velocity variation with depth: Geophysics, **58**, 1454–1467.

Levin, F., 1990, Reflection from a dipping plane—Transversely isotropic solid: Geophysics, **55**, 851–855.

Shearer, P. M. and Chapman, C. H., 1988, Ray tracing in anisotropic media with linear velocity gradient: Geophys. J. Internat., **94**, 575–580.

Thomsen, L., 1986, Weak elastic anisotropy: Geophysics, **51**, 1954–1966.

Tsvankin, I., and Thomsen, L., 1993, Nonhyperbolic reflection moveout in anisotropic media: Geophysics, in press.

Verwest, B. J., 1989, Seismic migration in elliptically anisotropic media: Geophysical Prospecting, **37**, 149–166.

FIGURE CAPTIONS

FIG. 1. Lateral position error, in terms of wavelengths (WL) at the reference frequency of 30 Hz, as a function of reflector dip in degrees (deg). ψ denotes the angle that the symmetry axis makes with the vertical. Black lines are for shale-limestone, and gray ones are for Cotton Valley shale (see Table 1). The solid lines show the error when migration velocity is based on the vertical rms velocity, and the dashed lines show the error when it is based on the best-fit stacking velocity. Vertical velocity gradient= 0.6 s^{-1}, here and throughout the paper, unless otherwise stated.

FIG. 2. Lateral position error as a function of reflector dip for two pairs of values for δ and ϵ. The vertical P-wave velocity function is the same for all the curves, but the velocity ratio V_s/V_p ranges from 0.3 to 0.7 in each figure.The symmetry axis is vertical (i.e., $\psi = 0$).

FIG. 3. Lateral position error as a function of reflector dip, for different combinations of ϵ and δ. Migration velocity is derived from the best-fit stacking velocity, and the axis of symmetry is vertical. The vertical velocity gradient $k = 0.6$ s^{-1}, and the reflection point is positioned at vertical migrated time $t_m = 2$ s.

FIG. 4. Lateral position error as a function of reflector dip and ϵ, for different values of vertical velocity gradient, k. Here $\delta = 0.05$, and the symmetry axis is vertical.

FIG. 5. Lateral position error as a function of reflector dip for different combinations of ϵ and δ. Migration velocity is derived from the vertical rms velocity, and the symmetry axis is vertical.

FIG. 6. Position error as a function of reflector dip and δ for different values of migrated time $t_m = 2D/V_{\rm rms}$, with $k = 0.6$ s^{-1}. Here $\epsilon = 0.1$, and the symmetry axis is vertical.

FIG. 7. Position error as a function of reflector dip and δ, for different orientations ψ of symmetry axis. Throughout, $\epsilon = 0.1$. In anticipation of Figure 11, the arrows point to approximately the position error for a reflector dip of 90 degrees in Taylor sandstone ($\delta = -0.035$ and $\epsilon = 0.11$).

FIG. 8. Position errors as a function of reflector dip for a medium where ϵ and δ vary with depth. At the surface the medium is isotropic, $\delta = \epsilon = 0$; at the reflector the medium is TI with $\epsilon = 0.1$ for the left plot, $\epsilon = 0.2$ for the right plot, and δ has the same values shown in Figure 6. Here, $\psi = 0$, and the gradient in vertical velocity is k=0.6 s^{-1}.

FIG. 9. Same as Figure 8, but this time the medium varies from being TI at the surface to isotropic at the reflector. Again k=0.6 s^{-1}.

FIG. 10. Model consisting of horizontal reflectors with segments having dips ranging from 30 to 90 degrees on both sides.

FIG. 11. Isotropic time migration of the model in Figure 10. (a): isotropic medium. (b) and (c): Taylor sandstone medium, with $\delta = -0.035$ and $\epsilon = 0.11$. In (b) the symmetry axis is vertical, and in (c) it is 30 degrees from the vertical. The vertical velocity $v(z)$=2000+0.6z m/s.

FIG. 12. Isotropic time migration of a simulated case of sedimentary beds upturned against the flank of a salt dome, where the medium is TI with (a) $\delta = 0.1$, $\epsilon = 0.15$ and $\psi = 0$, and (b) $\delta = -0.1$, $\epsilon = 0.1$ and $\psi = 0$. Both media have vertical velocity $v(z)$=2000+0.6z m/s. The correct reflector positions are represented by the dotted line.

FIG. 13. Depth migration of the reflector model in Figure 10. The medium is Taylor sandstone, with $\delta = -0.035$ and $\epsilon = 0.11$, where the axis of symmetry is vertical. The vertical velocity is $v(z)$=2000+0.6z m/s.

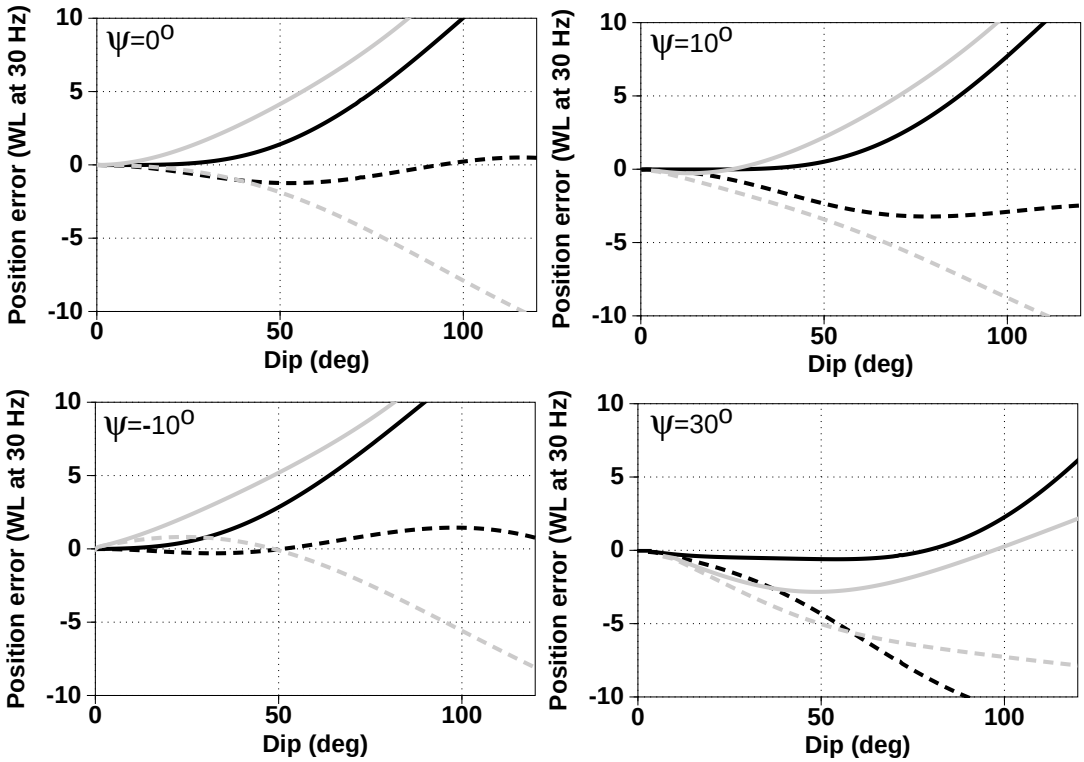
ψ=0°
ψ=10°
ψ=-10°
ψ=30°
Position error (WL at 30 Hz)
Dip (deg)
10
5
0
-5
-10
0
50
100

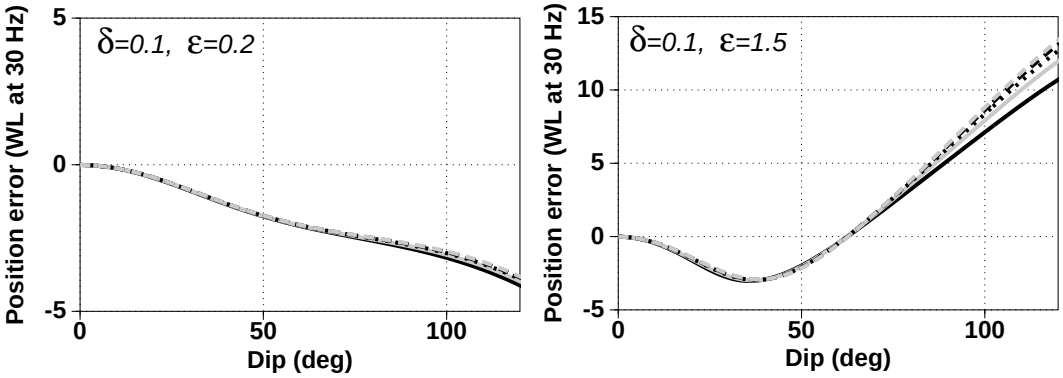
δ=0.1, ε=0.2
Position error (WL at 30 Hz)
5
0
-5
0
50
100
Dip (deg)
δ=0.1, ε=1.5
Position error (WL at 30 Hz)
15
10
5
0
-5
0
50
100
Dip (deg)

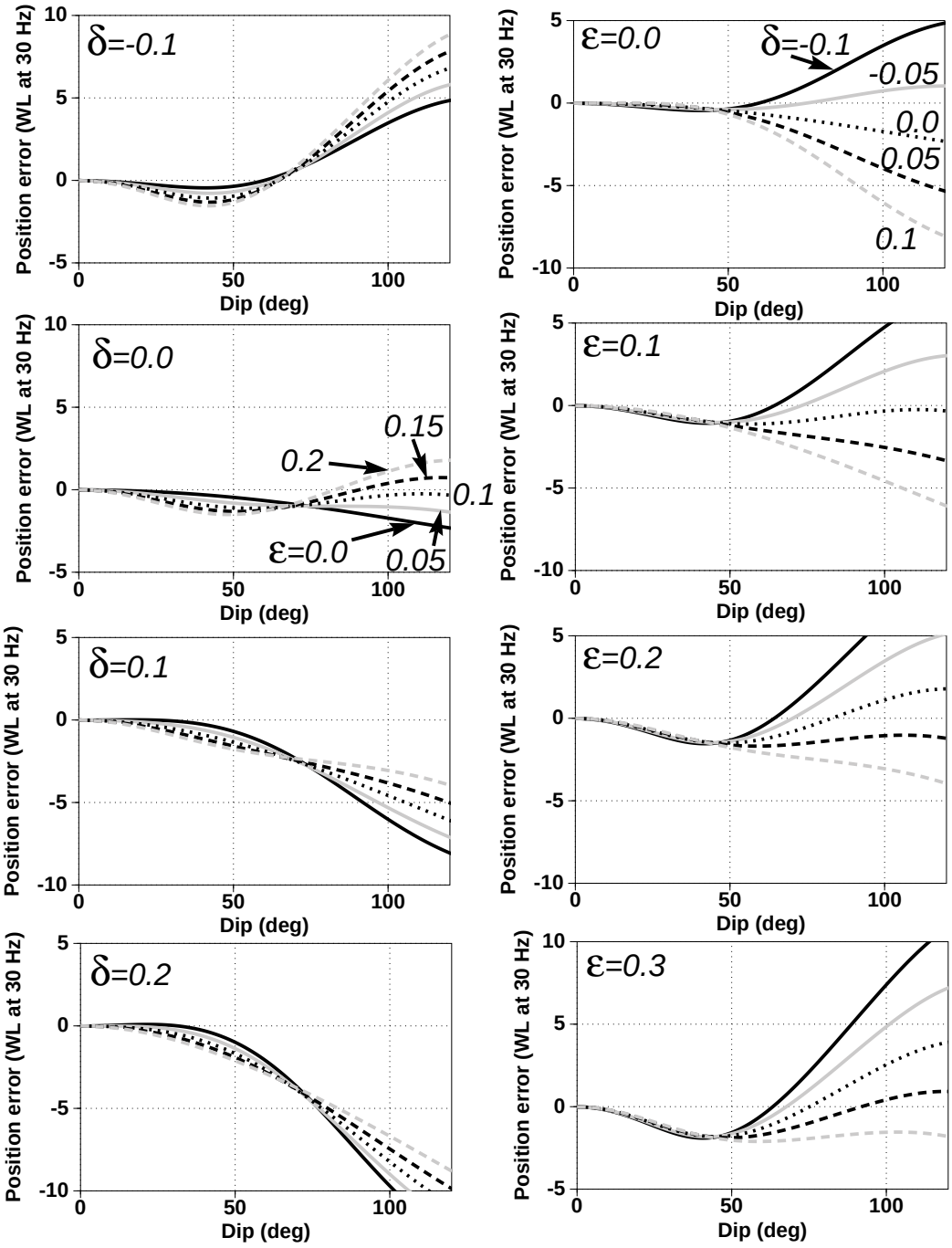
δ=-0.1
ε=0.0
δ=-0.1
-0.05
0.0
0.05
0.1
δ=0.0
0.15
0.2
0.1
ε=0.0
0.05
ε=0.1
δ=0.1
ε=0.2
δ=0.2
ε=0.3
Position error (WL at 30 Hz)
Dip (deg)

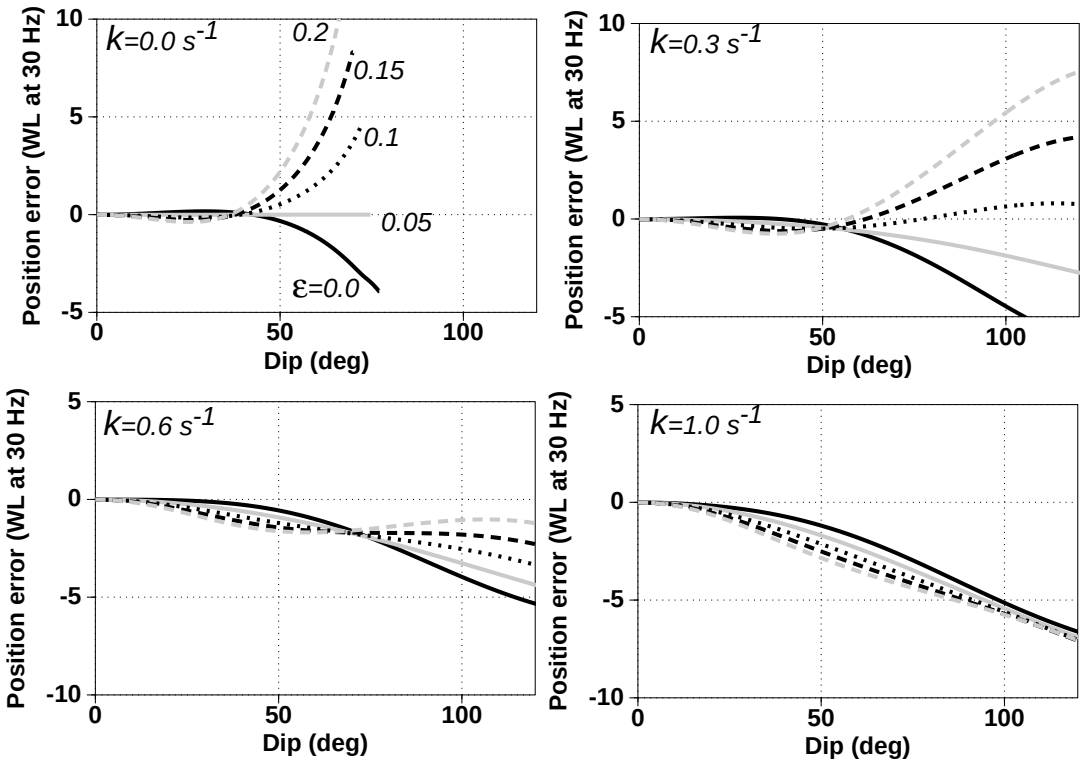
k=0.0 s-1
0.2
0.15
0.1
0.05
ε=0.0
k=0.3 s-1
k=0.6 s-1
k=1.0 s-1
Position error (WL at 30 Hz)
Dip (deg)
10
5
0
-5
-10
50
100

s

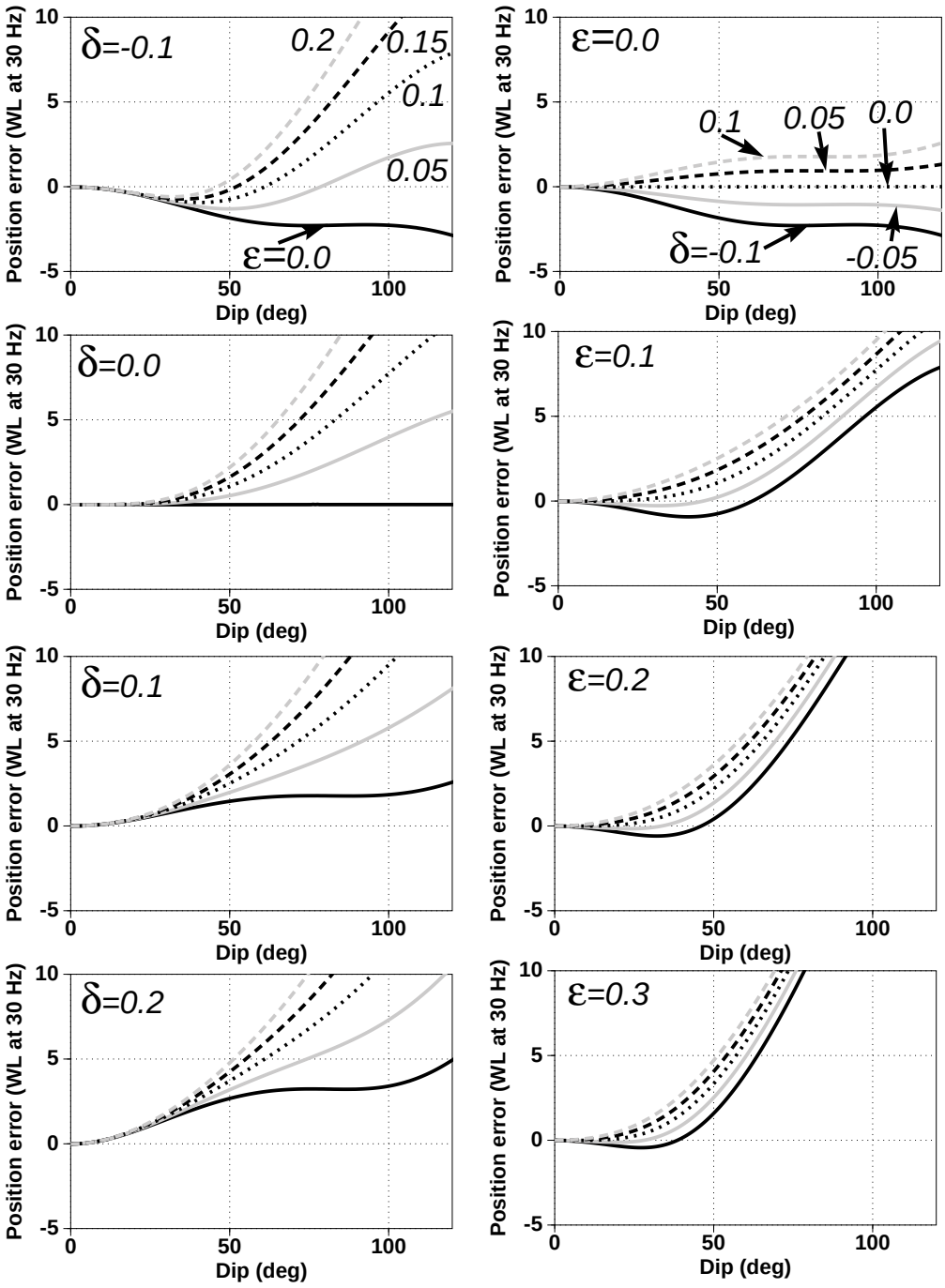
δ=-0.1
0.2
0.15
0.1
0.05
ε=0.0
ε=0.0
0.1
0.05
0.0
δ=-0.1
-0.05
δ=0.0
ε=0.1
δ=0.1
ε=0.2
δ=0.2
ε=0.3
Position error (WL at 30 Hz)
Dip (deg)
10
5
0
-5
0
50
100

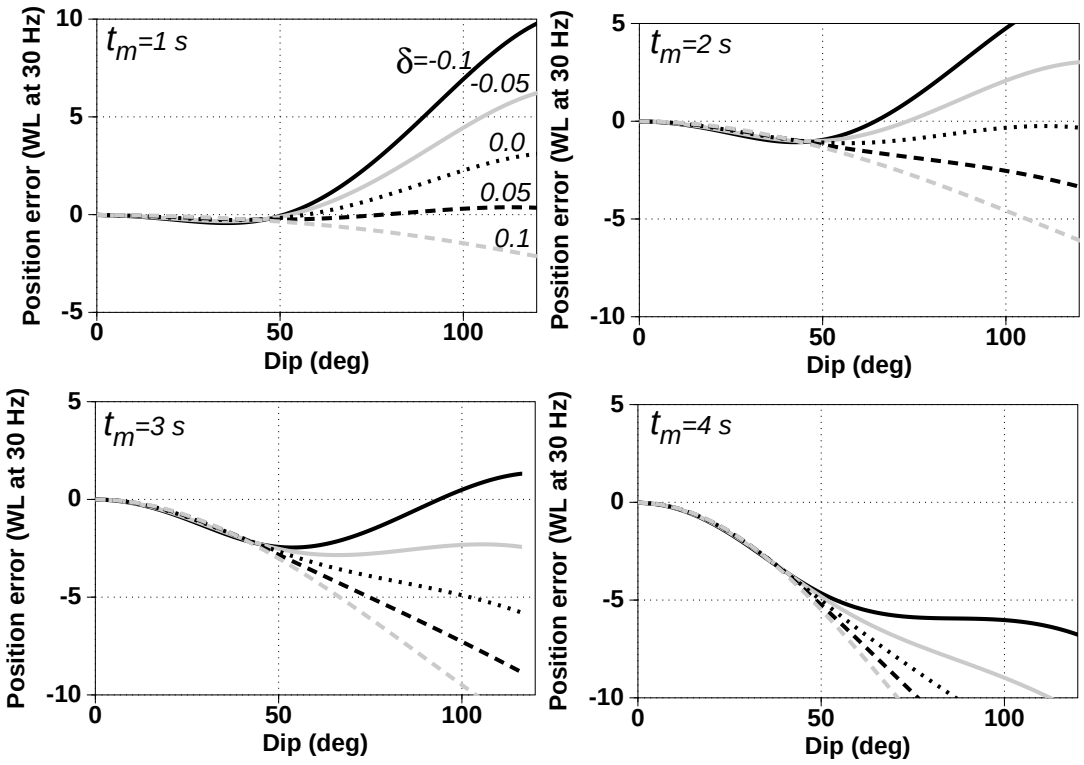
t_m=1 s
δ=-0.1
-0.05
0.0
0.05
0.1
Position error (WL at 30 Hz)
Dip (deg)
t_m=2 s
t_m=3 s
t_m=4 s

s

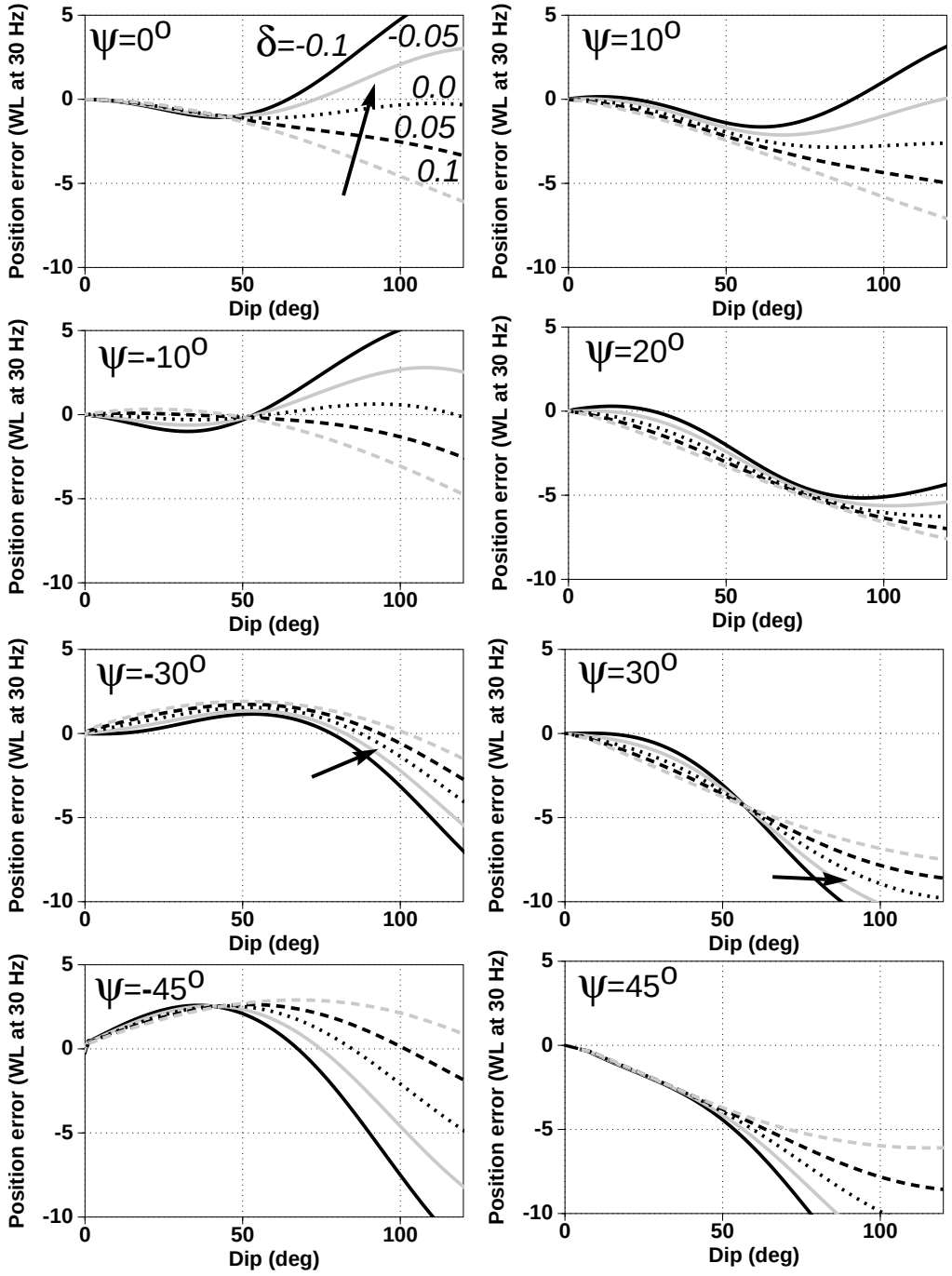
ψ=0°
δ=-0.1
-0.05
0.0
0.05
0.1
ψ=10°
ψ=-10°
ψ=20°
ψ=-30°
ψ=30°
ψ=-45°
ψ=45°
Position error (WL at 30 Hz)
Dip (deg)
5
0
-5
-10
0
50
100

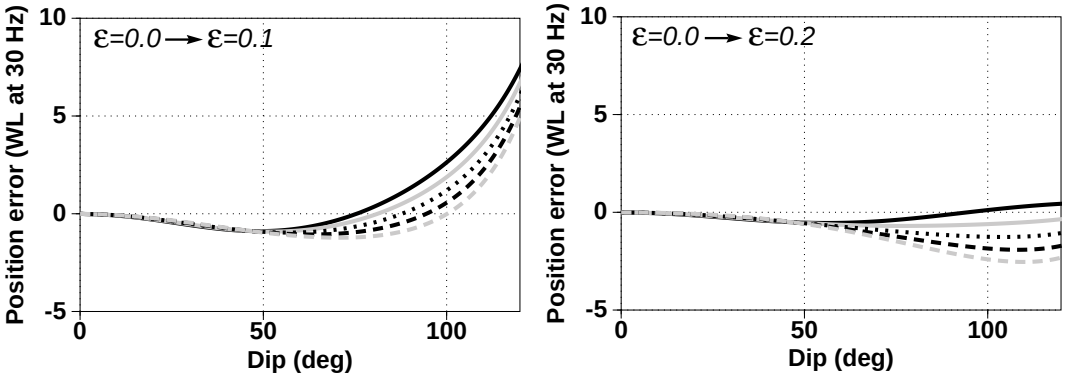
ε=0.0 → ε=0.1
Position error (WL at 30 Hz)
10
5
0
-5
0
50
100
Dip (deg)
ε=0.0 → ε=0.2
Position error (WL at 30 Hz)
10
5
0
-5
0
50
100
Dip (deg)

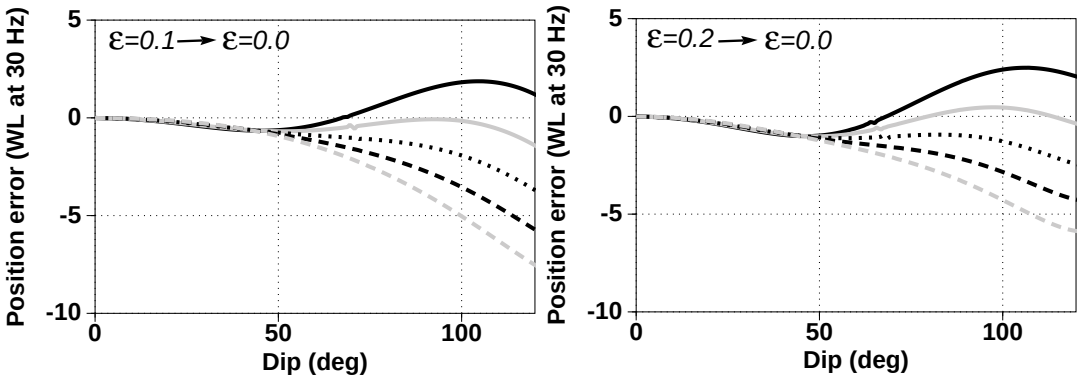
ε=0.1 → ε=0.0
ε=0.2 → ε=0.0
Position error (WL at 30 Hz)
Dip (deg)
5
0
-5
-10
0
50
100

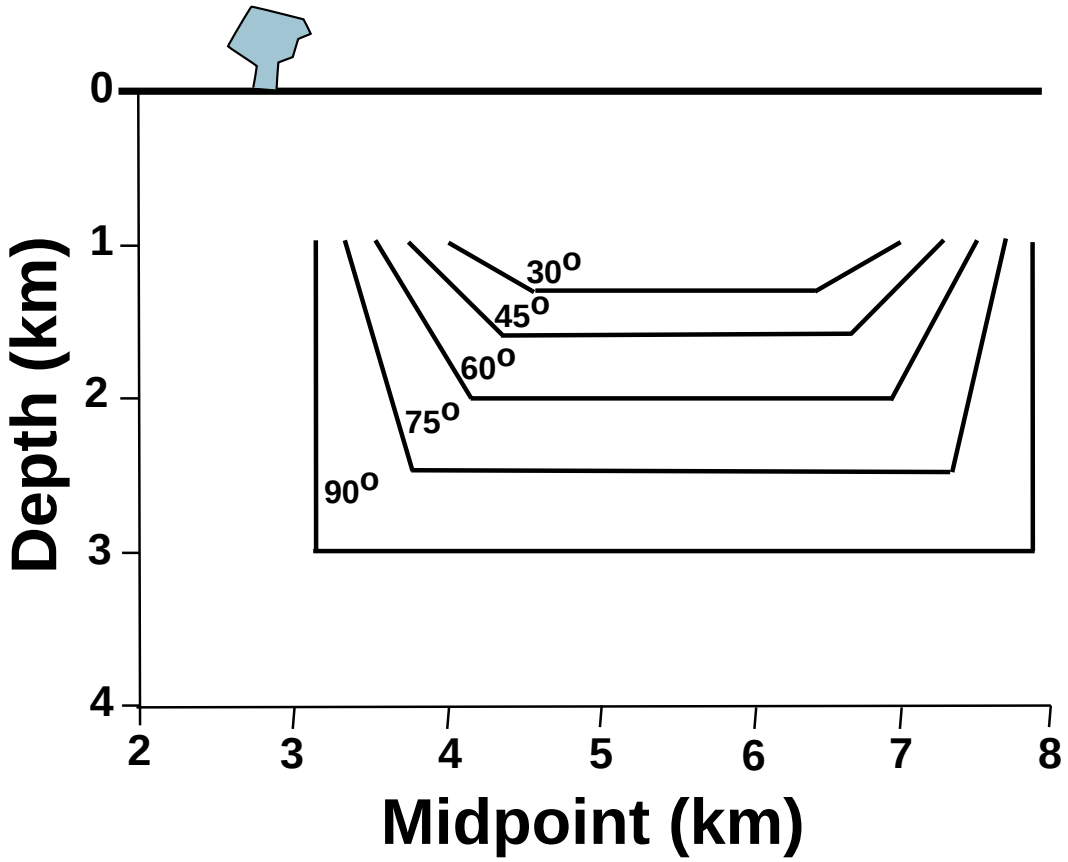
0
1
2
3
4
Depth (km)
30o
45o
60o
75o
90o
2
3
4
5
6
7
8
Midpoint (km)

Table 1. Thomsen's parameters δ and ε, along with the ratio of S-wave velocity to P-wave velocity V_s/V_p, for five TI media. The top four media listed are the same as those studied by Levin (1990); the Taylor sandstone was studied by Thomsen (1986).

Medium	$\frac{V_s}{V_p}$	δ	ε
Shale-limestone	0.55	0.0	0.134
Cotton Valley shale	0.61	0.205	0.135
Berea sandstone	0.63	0.02	0.002
Pierre shale	0.44	0.06	0.015
Taylor sandstone	0.54	-0.035	0.110

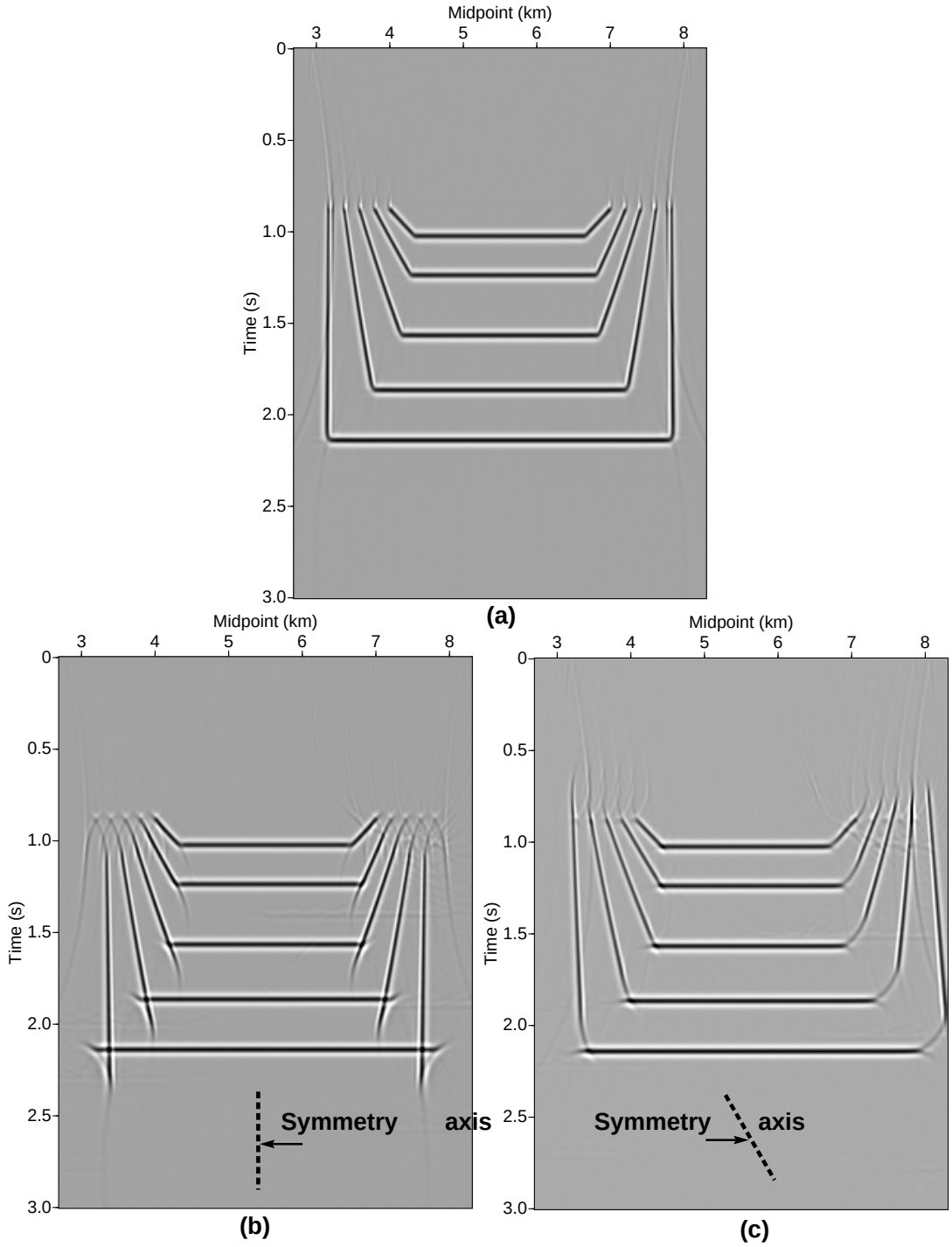
Midpoint (km)
3
4
5
6
7
8
0
0.5
1.0
1.5
2.0
2.5
3.0
Time (s)
(a)
Midpoint (km)
Time (s)
Symmetry axis
(b)
Midpoint (km)
Time (s)
Symmetry axis
(c)

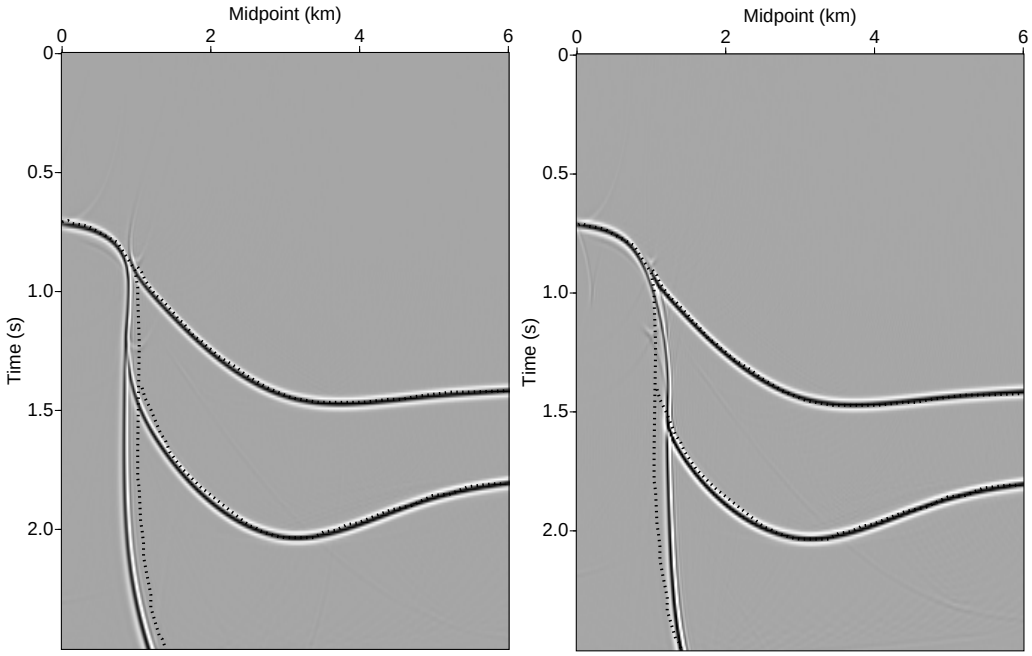
Midpoint (km)
0
2
4
6
0
0.5
1.0
1.5
2.0
Time (s)
Midpoint (km)
0
2
4
6
0
0.5
1.0
1.5
2.0
Time (s)

(a) **(b)**

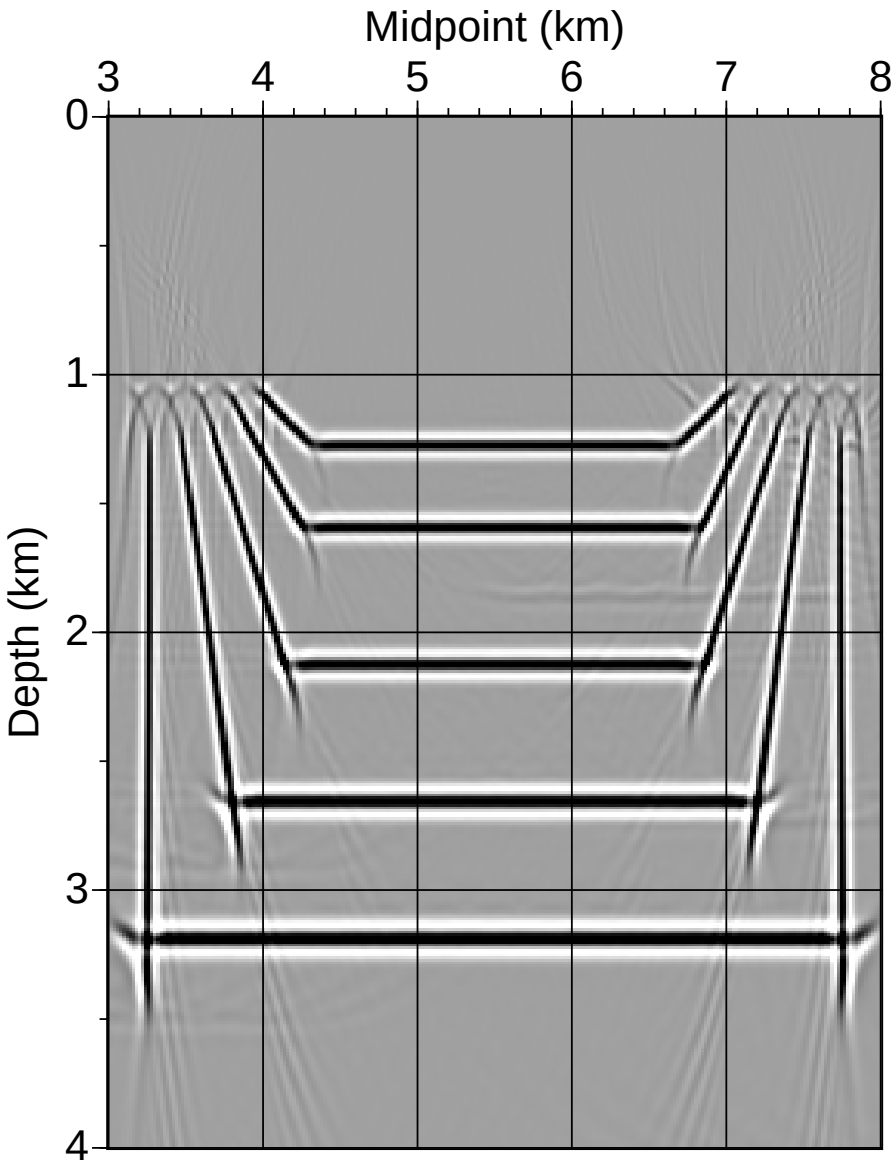
Midpoint (km)
3
4
5
6
7
8
0
1
2
3
4
Depth (km)

Table 2. Dependence of the ratio of the stacking to vertical rms velocity on the orientation of the symmetry axis for TI media. The spreadlength-to-depth ratio $X/D = 1.0$. $V_{\rm stack}$ is the stacking velocity corresponding to a $k = 0.6$ s^{-1} velocity gradient; the values for the ratio, $V_{\rm sh}/V_{\rm rms}(0)$, pertaining to homogeneous media with vertical symmetry axis, are those of Thomsen (1986) for $X/D \to 0$; and the number in parentheses denotes the angle between the vertical axis and the axis of symmetry.

Medium	$\frac{V_{\rm sh}}{V_{\rm rms}}(0)$	$\frac{V_{\rm stack}}{V_{\rm rms}}(0)$	$\frac{V_{\rm stack}}{V_{\rm rms}}(10)$	$\frac{V_{\rm stack}}{V_{\rm rms}}(20)$	$\frac{V_{\rm stack}}{V_{\rm rms}}(30)$	$\frac{V_{\rm stack}}{V_{\rm rms}}(45)$
Shale-limestone	1.00	1.07	1.08	1.09	1.10	1.07
Cotton Valley shale	1.19	1.17	1.15	1.11	1.06	0.99
Berea sandstone	1.02	1.02	1.02	1.01	1.01	1.00
Pierre shale	1.06	1.05	1.04	1.03	1.01	0.99
Taylor sandstone	0.96	1.04	1.05	1.08	1.10	1.08